

# Characteristic Study of Some Different Kinds of Coal Particles Combustion with Online TG-MS-FTIR

**Guanfu Pan**<sup>1,2,3</sup>

<sup>1</sup> China Coal Research Institute Company of Energy Conservation Corporation Ltd..

<sup>2</sup> State Key Laboratory of Coal Mining and clean Utilization.

<sup>3</sup> National Energy Technology & Equipment Laboratory of Coal Utilization and Emission Control.

Address of all above: 5 Qingniangou east road, Hepingli Subdistrict, Beijing, China.

Email: [panguanfubest@163.com](mailto:panguanfubest@163.com)

**Abstract.** Four kinds of pulverized coal samples from China and Indonesia were studied by thermogravimetry coupled with mass spectrometry and fourier transform infrared spectroscopy (TG-MS-FTIR). The thermal behaviors and gaseous emissions of these coals were analyzed in this work. The results indicate that the relative lower values of H/C ratios, which normally represent the degree of aromatization and ring condensation in coal samples, could lead to the relative more intense thermal reaction. The time-evolved profiles of some typical gas products (i.e., CO, SO<sub>2</sub>, CH<sub>4</sub>, NO, NO<sub>2</sub>, NH<sub>3</sub> and etc.) were provided by TG-MS-FTIR, and their variations are different. For all the samples, the releases of SO<sub>2</sub> and COS can be found at lower temperature than those of NO and CO. As the temperature increases, the possible conversion of NO<sub>2</sub> and NH<sub>3</sub> to NO is deduced in this work.

## 1. Introduction

Coal is an important and promising energy resource for electricity production due to its huge reserve in the world. At present, most power plants utilize the combustion of pulverized coal with fine particles below 100 μm to produce electricity [1]. In China, coal is the main source of primary energy and it accounts for about 70% of the total energy consumed [2]. Due to its huge reserves and lack of sufficient natural gas or oil reserves, coal will still be the main energy resource in China in the next decades. However, coal combustion leads to the increase of greenhouse gas emissions as well as air pollutants, such as nitrogen oxides (NO<sub>x</sub>), SO<sub>2</sub> and etc. Thus, understanding the kinetics and mechanisms during the combustion of pulverized coals is crucial to control the product composition.

Coal combustion involves lots of chemical reactions, including the cleavage of bridge bonds in the aromatic ring systems, the loss of heteroatom functional groups, and fragmentation of the macromolecular network [3]. The combustion of coal is affected by a series of factors, such as heating



rate, temperature and coal natures (i.e., coal type, particle size, chemical composition and etc.) [4-6]. Among these factors, coal properties are often considered as the key one before real application. Some traditional techniques and characteristic parameters, such as proximate and ultimate analysis, ash fusion temperatures and ash chemical composition, are commonly used to assess the behavior of pulverized coal during combustion. However, the test conditions of the above techniques are generally different from the real condition within a boiler or reactor, which sometimes would cause a large error [7]. To make good use of the pulverized coal, understanding of their thermal behavior is essential. The thermal analysis coupled to the measurement of evolved gas is very important to study the mechanism underlying coal combustion [8]. Recently, thermogravimetry coupled with mass spectrometry and Fourier transform infrared spectroscopy (TG-MS-FTIR) has been successfully used to study the thermal behavior and gaseous emission characteristic during the pyrolysis and combustion of specific coals [9-11]. The results indicate that TG-MS-FTIR is a very useful method, which integrates the advantages of TG, MS and FTIR. However, the systematic study on the effect of coals characteristic on their combustion behavior and evolved gases is rare.

The present work is oriented to study the thermal behaviors and gaseous emissions of four selected coal samples from different regions (SQ, YQ and DT are from China, YN is from Indonesia) by TG-MS-FTIR. The ignition and burnout temperature as well as the activation energy of the samples were deduced. Moreover, the information of the evolution of typical gaseous compounds during the combustion of the samples was revealed.

## 2. Experimental Methods

### 2.1. Samples

The coal samples were bought from Shenmu Energy Developments Ltd. Company and grinded into powder with particle size of 90~100  $\mu\text{m}$ . The results of proximate and ultimate analysis of the samples used in this work are listed in Table 1.

The  $M_{ad}$ ,  $A_{ad}$ ,  $V_{ad}$ , and  $FC_{ad}$  represent the moisture, ash, volatile and fixed carbon in air-dried basis, respectively. The  $C_{ad}$ ,  $H_{ad}$ ,  $O_{ad}$ ,  $N_{ad}$  and  $S_{ad}$  represent carbon, hydrogen, oxygen, nitrogen and sulfur elements in air-dried basis, respectively. H/C and O/C refer to the H/C and O/C atomic ratio, respectively.

**Table 1** The proximate and ultimate analysis results of four coal samples

Coal	Proximate analyses (wt.%)				Ultimate analysis (wt.%, daf)					H/C	O/C
	$M_{ad}$	$A_{ad}$	$V_{ad}$	$FC_{ad}$	$C_{ad}$	$H_{ad}$	$O_{ad}$	$N_{ad}$	$S_{ad}$		
SQ	6.50	18.98	27.13	47.39	59.26	3.29	10.34	0.86	0.77	0.67	0.13
YN	1.13	52.51	16.37	29.99	35.26	2.23	7.52	0.67	0.68	0.76	0.16
DT	0.88	34.90	6.39	57.83	59.80	1.20	1.67	0.92	0.63	0.24	0.02
YQ	0.60	14.42	2.70	82.28	80.71	1.16	0.92	1.13	1.06	0.17	0.01

### 2.2. TG-MS-FTIR Test

The experiments were performed with a TG analyzer (STA-449F3, Netzsch) coupled to a quadrupole mass spectrometer (QMS403C, Aeolos) and a FTIR spectrometer (Tensor 27, Bruker). About 10 mg of each sample was heated with a heating rate of 10  $^{\circ}\text{C}/\text{min}$  from 40 to 110  $^{\circ}\text{C}$  and kept for 30 min. Then, the samples were heated to 1070  $^{\circ}\text{C}$  at the heating rate of 20  $^{\circ}\text{C}/\text{min}$  in an atmosphere of 20 sccm  $\text{O}_2$  and 80 sccm Ar.

### 3. Results and Discussion

#### 3.1. TG Analysis

The TG and DTG curves of four coal samples are displayed in Figure. 1. As shown in Figure. 1a, the initial slopes of TG curves of SQ and DT are steeper than those of YQ and YN, showing that the thermal decomposition processes of SQ and DT occurred at lower temperatures than those of YQ and YN. From Figure. 1b, the rates of weight loss of SQ, DT, and YN are less than that of YQ. Therefore, the SQ and DT show more intense thermal reaction than YQ and YN. As can be seen from Table 1, the H/C atomic ratios of YN, SQ and DT are higher than that of YQ. It has been reported that the high H/C atomic ratio normally generate a low degree of aromatization and ring condensation in coal samples [3]. Thus, the SQ and DT are liable to suffer from thermal decomposition at lower temperatures than YQ who has relatively higher degree of aromatization and ring condensation. However, for the YN coal with the highest value of H/C atomic ratio, less intense thermal reaction was observed than SQ and DT, which is most likely caused by its highest ash content and O/C ratio among the four coal samples.

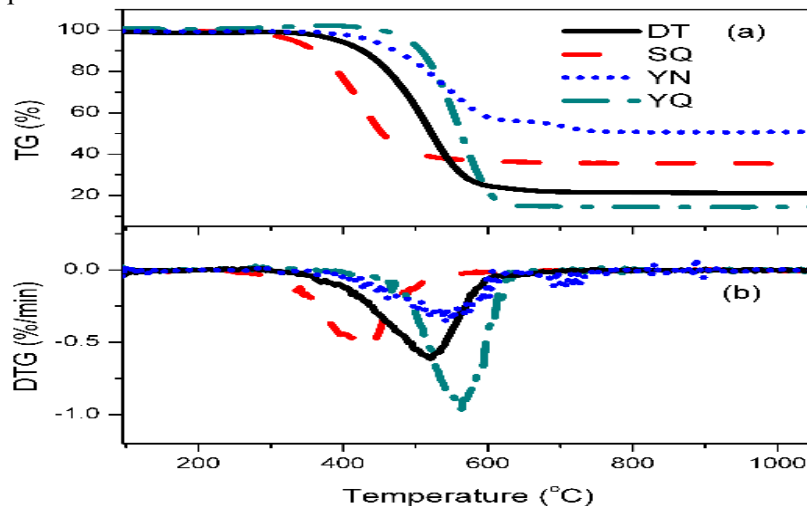


**Figure. 1** TG and DTG curves of four coal samples.

The characteristic temperatures and activation energies of the four coal samples are shown in Figure. 2. In this work, the ignition temperature ( $T_{ig}$ ) is determined by the commonly-used method [12]. The maximum reaction temperature ( $T_{max}$ ) refers to the temperature at which combustion products reach maximum volumetric flow. The burnout temperature ( $T_{burn}$ ) is defined as the temperature at 98% total weight loss. The activation energy is calculated by the Coats-Redfern method [13,14]. For the four coal samples, the orders of  $T_{ig}$  and  $T_{max}$  are consistent with that of activation energies. The  $T_{ig}$  and  $T_{max}$  as well as activation energies of SQ and DT are less than those of YN and YQ. The  $T_{burn}$  of YN is higher than that of other samples, which could be due to its highest ash contents. In fact, high ash contents will lead to the plugging of the surface pores and ash cladding, which would result in a higher burnout temperature.

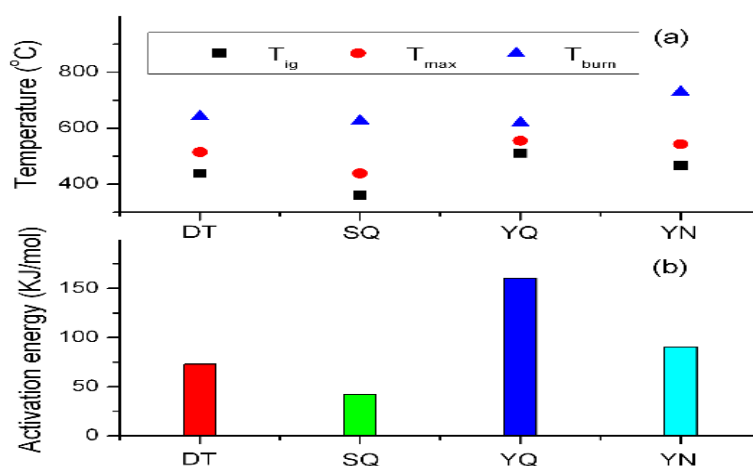


**Figure. 2** Characteristic temperatures and activation energies of four coal samples.

### 3.2. MS Analysis

Figure. 3 summarizes the time-evolved flowrates of some selected products during the combustion process of the four coal samples. The data was analyzed through calculation by taking into consideration the electron impact ionization cross sections, ion flow intensities and the partial pressures of different species [15].

For  $\text{CO}_2$ , it appears in the temperature range of 250 to 650 °C. At low temperature,  $\text{CO}_2$  comes mainly from the emission of adsorbed gas in the coal surface. With temperature increasing,  $\text{CO}_2$  is possibly from aromatic carboxyl or aliphatic groups [3]. At around 700 °C, a small amount of  $\text{CO}_2$  can be detected during YN coal combustion, which is possibly from oxygen-containing groups in YN coal [16]. The temperature range of CO is similar to that of  $\text{CO}_2$ , while the CO production is likely from the decomposition of carbonyl structures and phenolic groups in coal samples as temperature increases [17]. Among the four coal samples, the amounts of  $\text{CO}_2$  and CO emission from YQ are the highest, while those of YN are the lowest, which is consistent with the amount of carbon contents in the four coal samples (see Table 1).

The maximum temperatures of  $\text{SO}_2$  and COS emission are lower than each  $T_{max}$ , and the releases of  $\text{SO}_2$  and COS can be found at lower temperature than those of NO and CO. The curve of  $\text{SO}_2$  exhibits double peaks during YN and YQ coals combustion, which may result from the oxidation of aliphatic sulfur and aromatic sulfur components, respectively [18]. According to literatures [18-20], the formation of COS is mainly from the reaction of sulfur and CO generated in the combustion process.

For all samples, the formation of  $\text{CH}_4$  is detectable from 300 °C to above 650 °C. In fact, the temperature corresponding to the max flowrate is irregular for different samples. As shown in Figure. 3e, the temperature of max flowrate of YQ is higher than that of the other three samples, especially for SQ. The observation agrees with the previous discussion on the relationship of H/C atomic ratio and degree of aromatization. The  $\text{CH}_4$  produced at lower temperature results from the C-C bond cleavage between methyl and aliphatic chains or aromatic side chains [21]. At higher temperature, most of  $\text{CH}_4$  comes from the breakage of aryl-methyl group or aryl-alkyl ether bonds [3,22].

The  $\text{NH}_3$ , NO and  $\text{NO}_2$  are most likely from the decomposition of nitrogen components, such as nitrogen-containing heterocyclic species. The amounts of  $\text{NH}_3$ , NO and  $\text{NO}_2$  emissions from YQ are the highest among the four samples, which is due to its highest nitrogen contents. For all samples, it should be noted that the maximum temperature of  $\text{NO}_2$  and  $\text{NH}_3$  emission are lower than  $T_{max}$  of each

sample, while the maximum temperatures of NO emission are higher than each  $T_{\max}$ . Thus, the possible conversion of  $\text{NO}_2$  and  $\text{NH}_3$  to NO can be deduced as temperature increases during the combustion processes of the coal samples.

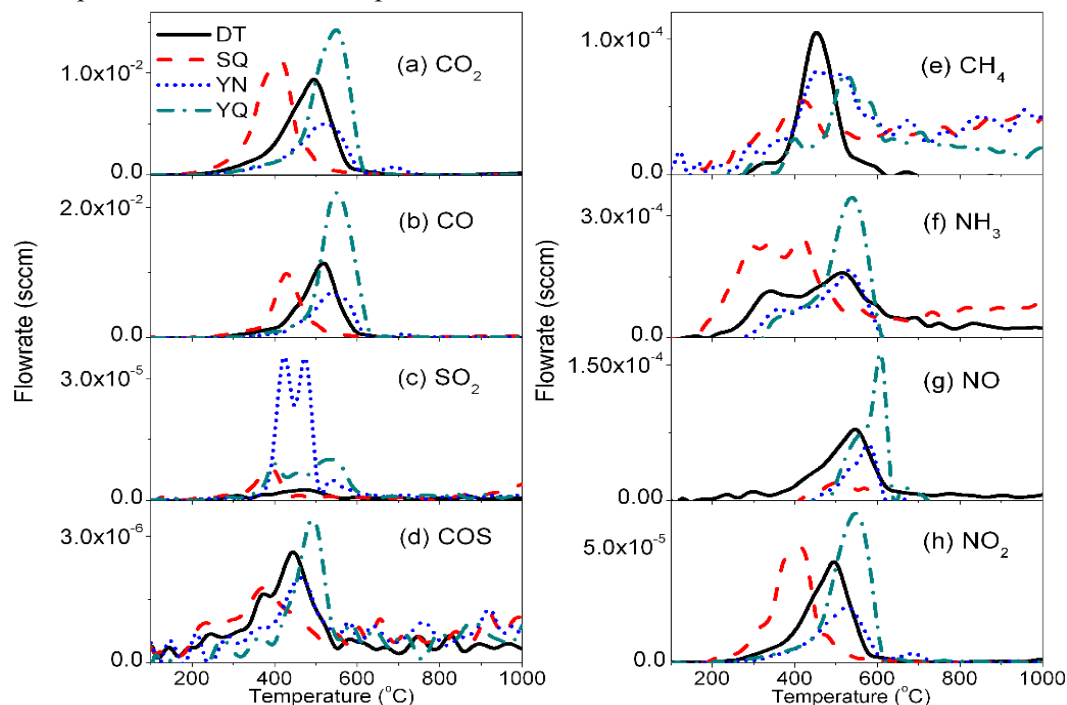


**Figure. 3** The time-evolved flowrates of some selected products during the combustion process of the four coal samples.

### 3.3. FTIR Analysis

To visualize the variations of the combustion products directly, FTIR analysis was performed. As the four samples exhibit similar behavior, only the three dimensional FTIR spectra during DT coal combustion (Figure. 4) is given here as a representative. The  $T_{\max}$  is consistent with the DTG curve of DT coal shown in Figure. 1b, which can also be observed during the combustion of the other coal samples (not shown).

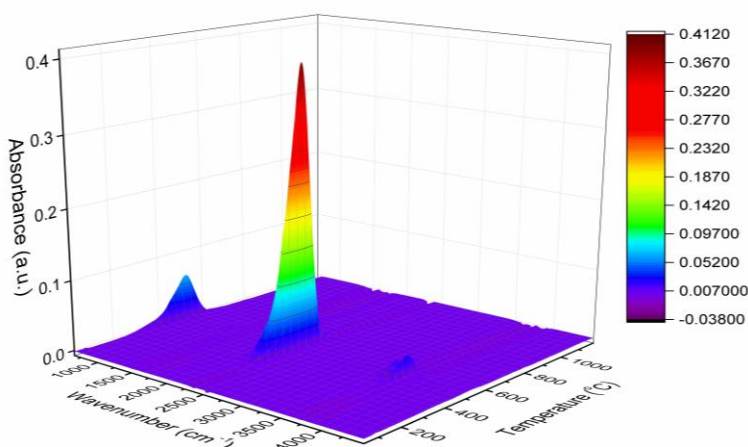


**Figure. 4** Three dimensional FTIR spectra during DT coal combustion.

The FTIR spectra during the combustion processes of four coal samples at different temperatures are shown in Figure. 5. The max absorbance bands at 2315-2380  $\text{cm}^{-1}$  come from  $\text{CO}_2$  [23]. CO was confirmed by the appearance of bands at 2180  $\text{cm}^{-1}$  and 2120  $\text{cm}^{-1}$  [24]. The bands at 1320-1400  $\text{cm}^{-1}$  and 1350-1500  $\text{cm}^{-1}$  are from  $\text{SO}_2$  and HCN, respectively [25]. The presence of  $\text{H}_2\text{O}$  is verified by the bands at 3550-3850  $\text{cm}^{-1}$  and 1500-1800  $\text{cm}^{-1}$ , which can hide the bands of some gases, such as NO (bands at 1500-1900  $\text{cm}^{-1}$ ),  $\text{NO}_2$  (bands at 1500-1700  $\text{cm}^{-1}$ ), and  $\text{NH}_3$  (bands at 1450-1800  $\text{cm}^{-1}$ ) [25]. At the temperature of 400  $^\circ\text{C}$ , the emissions of  $\text{CO}_2$ , CO, and  $\text{H}_2\text{O}$  from SQ are higher than those from other samples. As the temperature increases to 600  $^\circ\text{C}$ , the releases of  $\text{CO}_2$ , CO, and  $\text{H}_2\text{O}$  from YQ are the highest, while those from SQ are the lowest among the four coal samples, which can confirm the results discussed in the section of MS analysis.

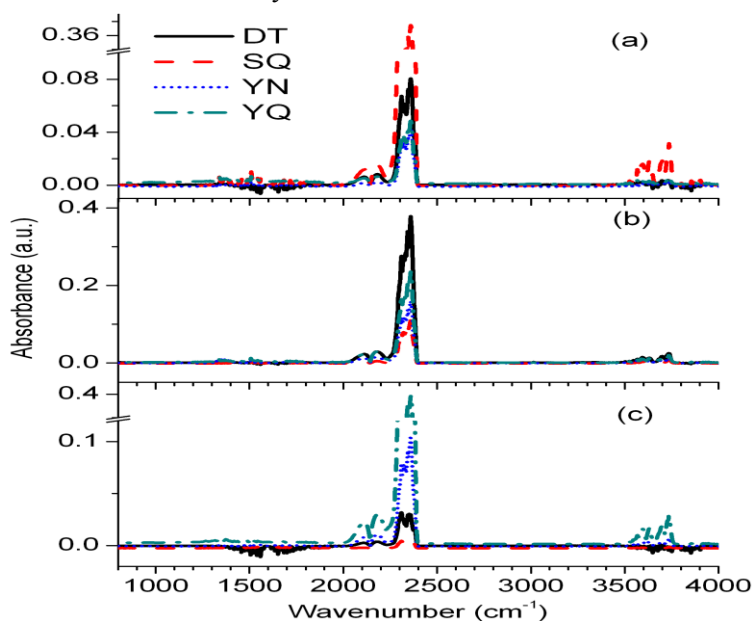


**Figure. 5** FTIR spectra during the combustion processes of four coal samples at different temperatures: (a) 400  $^\circ\text{C}$ , (b) 500  $^\circ\text{C}$ , and (c) 600  $^\circ\text{C}$ .

#### 4. Conclusions

The thermal behaviors and gaseous emissions of four selected coal samples from different regions were studied by TG-MS-FTIR. The results show that the SQ and DT exhibit more intense thermal reaction than YQ due to the relative lower degree of aromatization and ring condensation in SQ and DT than YQ, which normally can be deduced by the relative higher values of H/C ratios in SQ and DT than that in YQ. However, for the YN coal with the highest value of H/C ratio, less intense thermal reaction was observed than SQ and DT, which is most likely caused by its highest ash content and O/C ratio among the four coal samples. The information on the evolution of gaseous compounds, such as  $\text{CO}_2$ , CO,  $\text{SO}_2$ , COS,  $\text{CH}_4$ ,  $\text{NH}_3$ , NO, and  $\text{NO}_2$ , during the combustion of the coal samples were simultaneously obtained in this work. For all the samples, the releases of  $\text{SO}_2$  and COS can be found at lower temperature than those of NO and CO. As the temperature increases, the possible conversion of  $\text{NO}_2$  and  $\text{NH}_3$  to NO is deduced in this work. For coal samples with higher values of H/C atomic ratio, the gaseous products normally reach the max flowrates at lower temperatures. Thus, the release of gaseous compounds produced in the combustion processes is related to the different chemical structures and compositions in the coal samples.

## 5. Acknowledgments

The authors thank the financial support from the Natural Science Foundation of Beijing, China(Grant No. Z161100004816012).

## 6. References

- [1] S.M. Hwang, K. Oomagari, F.T. Akamatsu, M. Katsudi, R. Kurose, H. Tsuji, H. Makino, *Combustion Science and Technology in Asia-Pacific Area: Today and Tomorrow*, 2003, pp. 414-417.
- [2] R. Li, G.C.K. Leung, *Energ. Policy* 40 (2012) 438-443.
- [3] S.Q. Wang, Y.G. Tang, H.H. Schobert, Y.N. Guo, W.C. Gao, X.K. Lu, *J. Anal. Appl. Pyrol.* 100 (2013) 75-80.
- [4] P. Ghetti, *Fuel* 65 (1986) 636-639.
- [5] S. Kizgut, S. Yimaz, *Fuel Process. Technol.* 85 (2004) 103-111.
- [6] W. Zhu, W. Song, W. Lin, *Energy Fuels* 22 (2008) 2482-2487.
- [7] D.I. Barnes, *Appl. Therm. Eng.* 74 (2015) 89-95.
- [8] W. Xie, W.P. Pan, *J. Therm. Anal. Calorim.* 65 (2001) 669-685.
- [9] A. Arenillas, F. Rubiera, J.J. Pis, *Environ. Sci. Technol.* 36 (2002) 5498-5503.
- [10] A. Arenillas, C. Pevida, F. Rubiera, R. Garcia, J.J. Pis, *J. Anal. Appl. Pyrol.* 71 (2004) 747-763.
- [11] T. Kaljuvee, M. Keelman, A. Trikkel, V. Petkova, *J. Therm. Anal. Calorim.* 113 (2013) 1063-1071.
- [12] L.M. Lu, *Thermal Analysis in Practice*, Donghua University Press, 2010.
- [13] A.W. Coats, J.P. Redfern, *Nature* 201 (1964) 68-69.
- [14] A.W. Coats, J.P. Redfern, *J. Polym. Sci. Pol. Lett.* 3 (1965) 917-920.
- [15] H.D. Xia, K. Wei, *Thermochim. Acta*, 602 (2014) 15-21.
- [16] A. Arenillas, F. Rubiera, J.J. Pis, *J. Anal. Appl. Pyrol.* 50 (1999) 31-46.
- [17] K.H. Vanheek, W. Hodek, *Fuel* 73 (1994) 886-896.
- [18] W.H. Calkins, *Energy Fuels* 1 (1987) 59-64.
- [19] M. Fatemibedi, A.W. Scaroni, *Abstr. Pap. Am. Chem. Soc.* 195 (1988) 27.
- [20] P.A. Montano, P.P. Vaishnav, J.A. King, E.N. Eisentrout, *Fuel* 60 (1981) 712-716.
- [21] A. Arenillas, F. Rubiera, J.J. Pis, M.J. Cuesta, M.J. Iglesias, A. Jimenez, I. Suarez-Ruis, *J. Anal. Appl. Pyrol.* 68-69 (2003) 371-385.
- [22] W. Hodek, J. Kirschstein, K.H. Vanheek, *Fuel* 70 (1991) 424-428.
- [23] P.L. Gendreau, F. Vitaro, *Can. J. Publ. Health-Rev. Can. San.* 96 (2005) 167-172.
- [24] T. Ahamad, S.M. Alshehri, *J. Hazard. Mater.* 199 (2012) 200-208.
- [25] P.J. Linstrom, W.G. Mallard, *NIST Chemistry Webbook*. National Institute of Standard and Technology, Number 69, Gaithersburg, MD, <http://webbook.nist.gov/>, 2005.